PENERBIT
Universiti Sultan Zainal Abidin

MALAYSIAN JOURNAL OF APPLIED SCIENCES
eISSN:0127-9246

ORIGINAL ARTICLE

Effects of Heat Generation/Absorption on a Stagnation Point Flow Past a Stretching Sheet Carbon Nanotube Water-Based Hybrid Nanofluid with Newtonian Heating

Abdul Muiz Mohd Zaki[1], Nurul Farahain Mohammad[2], Siti Khuzaimah Soid[3], Muhammad Khairul Anuar Mohamed[1], Rahimah Jusoh[1]

[1]Centre for Mathematical Sciences, College of Computing & Applied Sciences, Universiti Malaysia Pahang, 26300 Gambang, Pahang, Malaysia
[2]Department of Computational and Theoretical Sciences, Kulliyyah of Science, International Islamic University Malaysia, Bandar Indera Mahkota, 25200 Kuantan, Pahang, Malaysia
[3]Faculty of Computer and Mathematical Sciences, Universiti Teknologi MARA, 40450 UiTM Shah Alam, Selangor, Malaysia

*Corresponding author: muizzacky@gmail.com

Abstract

This study investigates the mathematical modelling of heat generation/absorption effect on the convective flow of single wall carbon nanotube-copper (SWCNT-Cu)/water hybrid nanofluid towards a stagnation point past a stretching sheet with Newtonian heating. The set of governing equations in the form of non-linear partial differential equations are first transform using the similarity transformation technique then solved numerically by the Runge-Kutta-Fehlberg (RKF45) method in Maple software. The numerical solutions were obtained for the surface temperature, the heat transfer coefficient and the skin friction coefficient as well as the velocity and the temperature profiles. The features of the flow and heat transfer characteristics for various values of the stretching parameter, the conjugate parameter, the nanoparticle volume fraction parameter and the heat source/sink parameter are analyzed and discussed. It is found that effects of hybrid nanoparticles are more significant for lower stretching parameter and for large conjugate parameter values, as well as the heat generation/absorption.

Keywords: Carbon Nanotube, Hybrid Nanofluid, Newtonian Heating, Stagnation Point, Stretching Sheet

Introduction

Choi and Eastman (1995) proposed the term nanofluid (nanoparticles fluid suspension) to express thermodynamically stable suspensions of nanosized (1–100 nm) solid particles in same base fluids as water and ethylene glycol. Nanofluids, which are made by disseminating nanoparticles into conventional heat transfer fluids, have been recommended as the future heat transfer fluids because they provide intriguing new possibilities for improving heat transfer performance above conventional fluids.

Nanofluids were shown to have significantly enhanced thermal characteristics, particularly thermal conductivity, even when suspended nanoparticle concentrations were relatively low, according to experiments reported by many researchers over the last decade (Chandrasekar et al., 2010; S. Choi et al., 2001; Eastman et al., 1996; Li & Peterson, 2006; Wang et al., 1999; Xuan et al., 2003; Zhu et al., 2006). The addition of nanoparticles considerably improves the heat transfer capability of the base fluids such as water and organic liquids including polymeric solutions, oil and lubricants. In addition, nanometer-sized particles dispersed in single-phase fluids have a larger specific surface area than colloidal suspensions and are more stable than ordinary slurries (Sundar et al., 2017).

Consequently, this type of nanostructured materials is extremely expensive and difficult to mass-produce. As a result, the utilisation of oxide nanoparticles is more cost-effective. According to the developmental study on nanofluids, adding a little number of metal nanoparticles and oxide nanoparticles suspended in a based-fluid can considerably increase the thermal characteristics (Mohamed et al., 2020). Researchers in the field of nanofluid heat transfer have recently embraced the usage of hybrid nanofluids. Due to the decrease in the price of nanofluids and the increase in their efficiency, this notion has been accepted. In comparison to oxide nanofluid, the hybrid nanofluid has a greater effective thermal conductivity and heat transport properties than metal nanofluid while having a cheaper production cost. According to Esfe et al. (2017), in addition to providing a desirable and high thermal conductivity, hybrid nanofluids can reduce the expensive price of nanofluids containing carbon nanotubes (CNT) while also ensuring sufficient and acceptable stability, laying the framework for large industrialization.

When it comes to the stretching sheet activity in the manufacturing process, the stretching rate and the heat transfer rate on the stretching sheet play a significant role in the final product's quality. Crane (1970) was the first to investigate convection flow through a stretching sheet. The research on the flow of a stretching sheet was then expanded to include various fluid types such as viscoelastic fluid, nanofluid, micropolar fluid, Jeffrey fluid, Cassonfluid, and ferrofluid in the stagnation area (Alkasasbeh et al., 2019; Bachok et al., 2011; Hamid et al., 2016; Hayat et al., 2016; Ishak et al., 2019; Noor et al., 2015; Yacob et al., 2011; Yasin et al., 2019). With the addition of other external factors such as thermal radiation, chemical reaction, slip flow, viscous dissipation, suction/injection, the magnetohydrodynamic (MHD) field, and Newtonian heating boundary conditions, this issue is getting more appealing year by year (Chamkha et al., 2015; Hashim et al., 2015; Hsiao, 2016; Mabood et al., 2016; Mohamed et al., 2019).

Due to the cost and difficulty of conducting an experimental research on this topic, the mathematical model was employed as a starting point for the investigation. This process is low-cost, fast, and gives fundamental understanding of the hybrid nanofluid, allowing for the prediction of early fluid flow and heat transfer characteristics. As a result of the previous literature, the purpose of this study is to examine the fluid flow and heat characteristics of single wall carbon

nanotube (*SWCNT)* nanoparticles blended with copper, *Cu* in water-based hybrid nanofluid at a stagnation point over a stretching sheet paired with Newtonian heating.

Materials and Methods

Mathematical Formulation

A steady two-dimensional steady flow on a stagnation point across a stretching sheet immersed in an incompressible viscous fluid of ambient temperature, T_∞ are depicted as physical model and coordinate system in Figure 1. The stretching velocity $u_w(x)$ and the free stream velocity $U_\infty(x)$ are assumed to have the forms $u_w(x) = ax$ and $U_\infty(x) = bx$, respectively, where a and b are constants. As proposed by Merkin (Merkin, 1994), the sheet is also supposed to be subjected to Newtonian heating boundary conditions. The equations for the boundary layer are as follows:

$$\frac{\partial u}{\partial x} + \frac{\partial v}{\partial y} = 0 , \tag{1}$$

$$u\frac{\partial u}{\partial x} + v\frac{\partial v}{\partial y} = U_\infty \frac{dU_\infty}{dx} + v_{hnf}\frac{\partial^2 u}{\partial y^2}, \tag{2}$$

$$u\frac{\partial T}{\partial x} + v\frac{\partial T}{\partial y} = \frac{k_{hnf}}{(\rho C_p)_{hnf}}\frac{\partial^2 T}{\partial y^2} + \frac{Q_o}{(\rho C_p)_{hnf}}(T - T_\infty). \tag{3}$$

subject to the boundary conditions

$$u = u_w , v = 0 , \frac{\partial T}{\partial y} = -h_s T , \text{ at } y = 0,$$

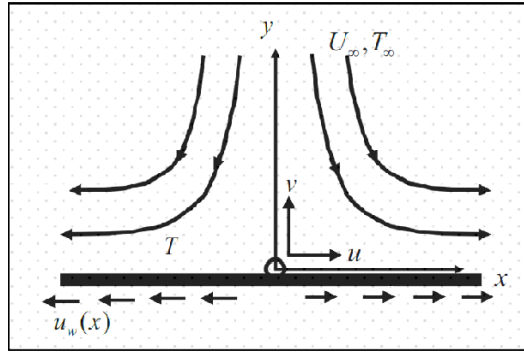$$u \to U_\infty , T \to T_\infty , \text{ as } y \to \infty. \tag{4}$$

Figure 1: Coordinate system and physical model

The kinematic viscosity, dynamic viscosity, and density of a hybrid nanofluid are indicated by the letters v_{hnf}, μ_{hnf}, and ρ_{hnf} accordingly. T is the temperature inside the boundary layer, $(\rho C_p)_{hnf}$ is the hybrid nanofluid's heat capacity, k_{hnf} is the hybrid nanofluid's thermal conductivity and Q_o is the dimensional heat generation or absorption coefficient. Other properties of the base fluid and nanoparticles are represented by the subscript $_f$ and $_{s1,s2}$ correspondingly as the following (Devi & Devi, 2017):

$$v_{hnf} = \frac{\mu_{hnf}}{\rho_{hnf}} , \ \rho_{hnf} = (1-\phi_2)[(1-\phi_1)\rho_f + \phi_1\rho_{s1}] + \phi_2\rho_{s2} , \ \mu_{hnf} = \frac{\mu_f}{(1-\phi_1)^{2.5}(1-\phi_2)^{2.5}} ,$$

$$(\rho C_p)_{hnf} = (1-\phi_2)[(1-\phi_1)(\rho C_p)_f + \phi_1(\rho C_p)_{s1}] + \phi_2(\rho C_p)_{s2} , \tag{5}$$

$$\frac{k_{hnf}}{k_{bf}} = \frac{k_{s2} + 2k_{bf} - 2\phi_2(k_{bf} - k_{s2})}{k_{s2} + 2k_{bf} + \phi_2(k_{bf} - k_{s2})} , \ \frac{k_{bf}}{k_f} = \frac{k_{s1} + 2k_f - 2\phi_1(k_f - k_{s1})}{k_{s1} + 2k_f + \phi_1(k_f - k_{s1})} .$$

Where ϕ_1, ϕ_2 are the volume fractions of nanoparticles for *SWCNT* and *Cu*, respectively. To make *Cu/water* nanofluid, solid nanoparticles of *Cu* (ϕ_2 =0.1) are mixed into a water-based fluid. Then, the solid nanoparticle of *SWCNT* (ϕ_1 = 0.06) is then added to the *Cu/water* nanofluid to create the *SWCNT—Cu /water* hybrid nanofluid. It's worth noting that equations (1), (2) and (3) are nonlinear partial differential equations with a large number of dependent and independent variables. It is also in dimensional forms, which increasing the difficulty of solving the equation directly. As a result, the similarity transformation method is used:

$$\eta = \left(\frac{b}{v_f}\right)y , \ \psi = (bv_f)^{1/2} xf(\eta) , \ \theta(\eta) = \frac{T - T_\infty}{T} . \tag{6}$$

The similarity variables are shown in Equation (6), where ψ and θ are non-dimensional variables, stream function, and temperature, respectively. The similarity variables (6) identically satisfy the continuity equation (1). Thus,

$$u = \frac{\partial \psi}{\partial y} \text{ and } v = -\frac{\partial \psi}{\partial x}. \tag{7}$$

By substituting the similarity variables equation in (6) and (7) into governing equations (2) and (3), the transformed ordinary differential equations can be yield as follow:

$$\frac{1}{(1-\phi_1)^{2.5}(1-\phi_2)^{2.5}[(1-\phi_2)[(1-\phi_1)+\phi_1(\rho_{s1}/\rho_f)]+\phi_2(\rho_{s2}/\rho_f)]} f''' + ff'' - f'^2 + 1 = 0 \tag{8}$$

$$\frac{k_{hnf}/k_f}{(1-\phi_2)[(1-\phi_1)+\phi_1(\rho C_p)_{s1}/(\rho C_p)_f]+\phi_2(\rho C_p)_{s2}/(\rho C_p)_f} \theta'' + \Pr f\theta' + \Pr \lambda\theta = 0 \tag{9}$$

Where prime denotes differentiation with respect to η and $\Pr = \dfrac{v_f(\rho C_p)_f}{k_f}$ is the Prandtl number which has constant value of 6.2 with respect to water-based fluid. Meanwhile, $\gamma = h_s\left(\dfrac{b}{v_f}\right)$ is the conjugate parameter, $\lambda = \dfrac{Q_o}{b\rho C_p}$ is the heat source $(\lambda > 0)$ or heat sink $(\lambda < 0)$ parameter, and $\varepsilon = \dfrac{a}{b}, (\varepsilon > 0)$ is the stretching parameter used. The boundary conditions (4) becomes

$$f(0) = 0, \ f'(0) = \varepsilon, \ \theta'(0) = -\gamma(1+\theta(0)),$$
$$f'(\eta) \to 1, \ \theta(\eta) \to 0, \text{ as } y \to \infty. \tag{10}$$

The physical quantities involved are the heat transfer rate $-\theta'(0)$, the surface temperature $\theta(0)$ and the skin friction coefficient C_f which given by

$$C_f = \frac{\tau_w}{\rho_f U_\infty^2}, \tag{11}$$

38

where the surface shear stress $\tau_w = \mu_{hnf} \left(\dfrac{\partial u}{\partial y} \right)_{y=0}$. The skin friction coefficient C_f can be reduced to

$$C_f \, \mathrm{Re}_x^{1/2} = \frac{f''(0)}{(1 - \phi_1)^{2.5} (1 - \phi_2)^{2.5}} , \tag{12}$$

as Reynolds number denoted by $\mathrm{Re}_x = \dfrac{U_\infty x}{v_f}$.

Results and Discussion

The Runge-Kutta-Fehlberg (RKF45) approach was used to solve the system of ordinary differential equations (8) and (9) with boundary conditions (10) numerically. The numerical results are obtained for the surface temperature $\theta(0)$, the heat transfer rate $-\theta'(0)$, and the reduced skin friction coefficient $C_f \, \mathrm{Re}_x^{1/2}$ for various values of stretching parameter ε , conjugate parameter γ , the nanoparticle volume fractions for *SWCNT* ϕ_1 and *Cu* ϕ_2 , and the heat source/sink parameter λ . Prandtl number Pr is fixed to 6.2 for each numerical analysis. To compute, the boundary layer thickness are set ranging from 3 to 7 for *Cu/water* nanofluid, and *SWCNT—Cu/water* hybrid nanofluid. Table 1 lists the values of thermophysical characteristics of water and nanoparticles that were taken into account.

Table 1: Thermophysical properties of water and nanoparticles

Physical Properties	Water (f)	SWCNT(ϕ_1)	Cu (ϕ_2)
$\rho \left(\dfrac{kg}{m^3} \right)$	997	2600	8953
$C_p \left(\dfrac{J}{kg \cdot K} \right)$	4179	425	385
$k \left(\dfrac{W}{m \cdot K} \right)$	0.613	6600	400

To validate the effieciency of the method used, the comparison of present and previous numerical results was performed. Table 2 displays the $C_f \, \mathrm{Re}_x^{1/2}$ values compared to Bachok et al. (2011), Yacob et al. (2011) and Mohamed et al. (2020) as previous results. The numerical results of present study is validated with the previous reporting.

Table 2: Comparison $C_f \mathrm{Re}_x^{1/2}$ values for specific values of ε and ϕ_1 (Al_2O_3) with previous results as $\mathrm{Pr} = 6.2, \lambda = \phi_2 = 0$ and $\gamma = 1$.

ε	ϕ_1	Bachok et al. (2011)	Yacob et al. (2011)	Mohamed et al. (2020)	Present
0	0.1	1.6019	1.6019	1.602081	1.602081384
	0.2	2.0584	2.0584	2.058376	2.058376034
0.5	0.1	0.9271	—	0.927121	0.927120763
	0.2	1.1912	—	1.191179	1.191176331

1
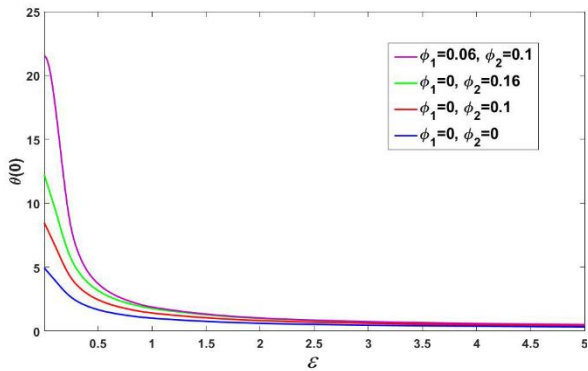
Figure 2: Variation of ε yielding profuse values of $\theta(0)$ when $\mathrm{Pr} = 6.2$, $\lambda = 0.1$ and $\gamma = 1$.
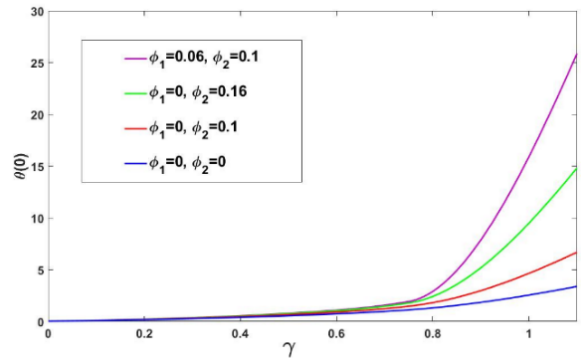

Figure 4: Variation of γ yielding profuse values of $\theta(0)$ when $\mathrm{Pr} = 6.2$, $\lambda = 0.1$ and $\varepsilon = 0.5$.
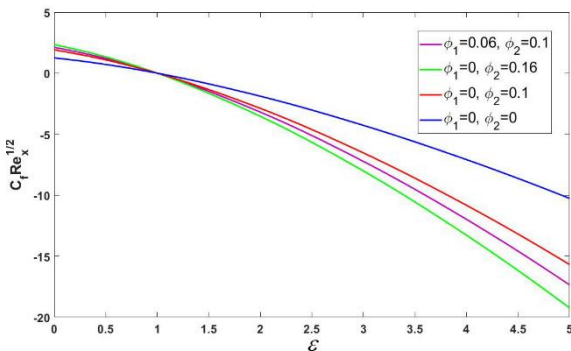

Figure 3: Variation of ε yielding profuse values of $C_f \mathrm{Re}_x^{1/2}$ when $\mathrm{Pr} = 6.2$, $\lambda = 0.1$ and $\gamma = 1$.
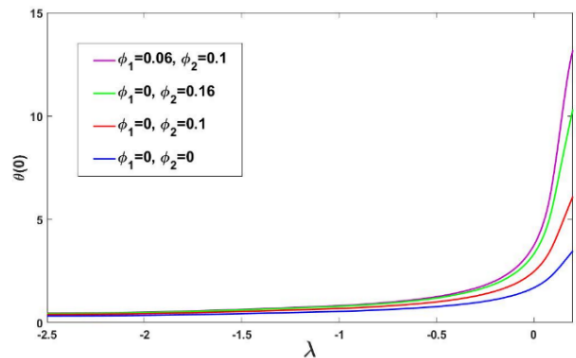

Figure 5:. Variation of λ yielding profuse values of $\theta(0)$ when $\mathrm{Pr} = 6.2$, $\gamma = 1$ and $\varepsilon = 0.5$.

Correlation of $\theta(\eta)$ ***and*** $f'(\eta)$ ***for Various*** ε **,** γ **and** λ
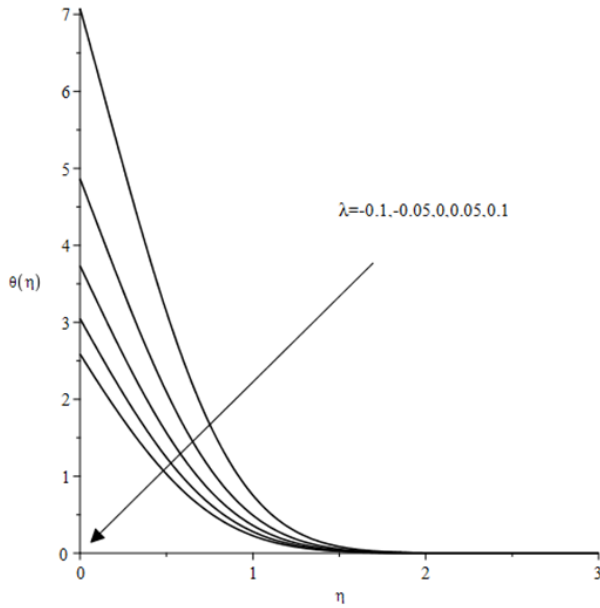

Figure 6: Temperature profiles $\theta(\eta)$ for various λ when $\mathrm{Pr} = 6.2$, $\gamma = 1$ and $\varepsilon = 0.5$.
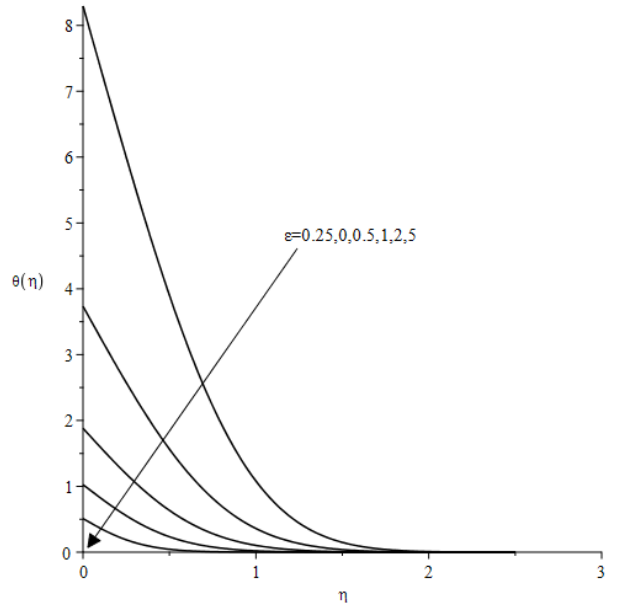
Figure 8: Temperature profiles $\theta(\eta)$ for various ε when $\mathrm{Pr} = 6.2$, $\lambda = 0.1$ and $\gamma = 1$.
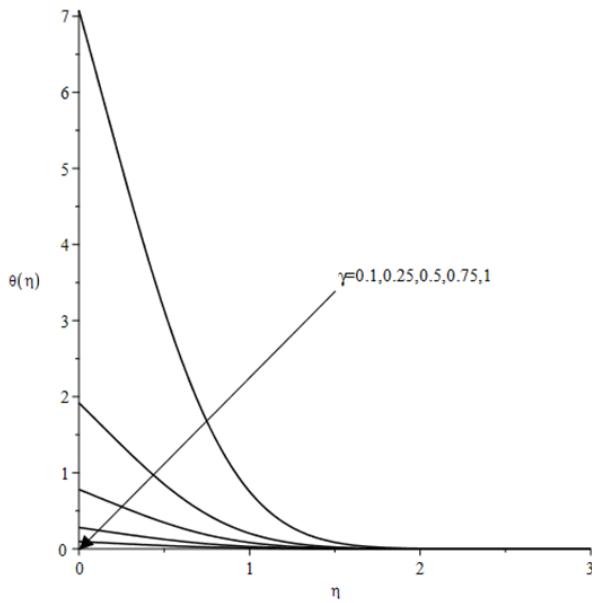

Figure 7: Temperature profiles $\theta(\eta)$ for various γ when $\mathrm{Pr} = 6.2$, $\lambda = 0.1$ and $\varepsilon = 0.5$.
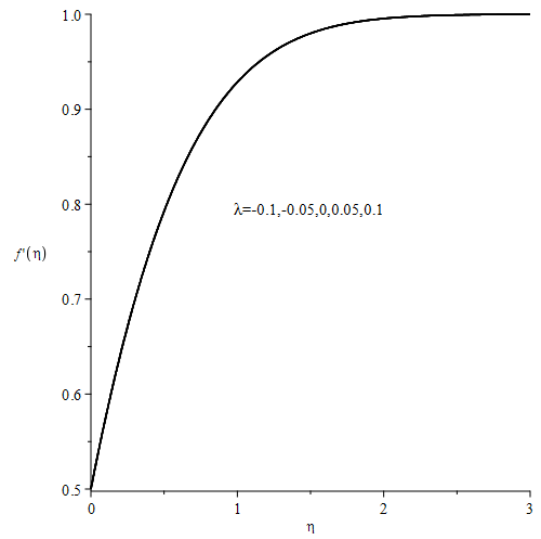

Figure 9: Velocity profiles $f'(\eta)$ for various λ when $\mathrm{Pr} = 6.2$, $\gamma = 1$ and $\varepsilon = 0.5$.
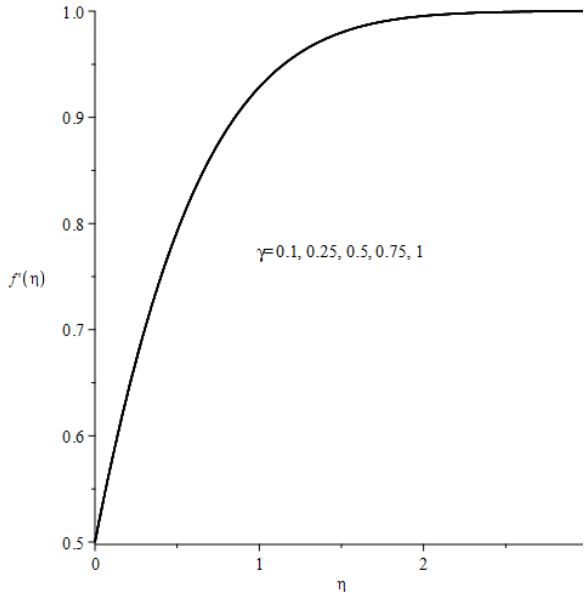
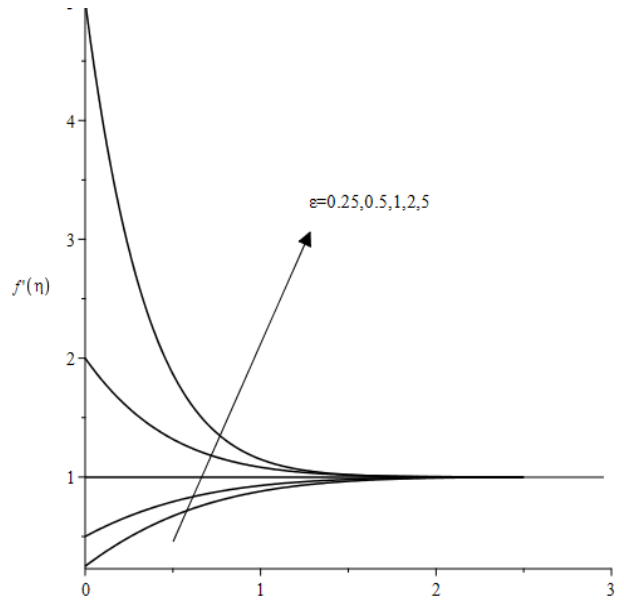Figure 10: Velocity profiles $f'(\eta)$ for various γ when $\mathrm{Pr}=6.2$, $\lambda=0.1$ and $\varepsilon=0.5$.

Figure 11: Velocity profiles $f'(\eta)$ for various ε when $\mathrm{Pr}=6.2$, $\lambda=0.1$ and $\gamma=1$.

The relationship of variation of the stretching parameter against various surface temperature is revealed in Figure 2. The surface temperature $\theta(0)$ decreases as the stretching parameter value ε increases. In terms of the influence of nanoparticles in fluid, Figure 2 shows that when 0.1 vol. of *Cu* nanoparticles is added to a water-based fluid to form a *Cu/water* nanofluid, the surface temperature rises. In similar trend yet more significant, when *SWCNT* nanoparticles are added to *Cu/water* to produce the *SWCNT—Cu/water* hybrid nanofluid, the temperature rises dramatically. However, the rise in surface temperature for the 0.16 vol. *Cu/water* nanofluid is less notable compared to the *SWCNT—Cu/water* hybrid nanofluid. At a tiny ratio of stretching parameter over free stream velocity, the impacts of hybrid nanoparticles are more noticeable. As stretching parameter increases $(\varepsilon>1)$, the differences become insignificant.

Figure 3 shows the effect of distinction of volume fractions of nanoparticles ϕ and hybrid nanofluid on the variation of the reduced skin friction coefficient $C_f \, \mathrm{Re}_x^{1/2}$ against various values of stretching parameter ε. Skin friction is generally positive from $0<\varepsilon<1$ and subsequently becomes negative $\varepsilon>1$ due to changes in velocity direction as mentioned in boundary conditions (4). $C_f \, \mathrm{Re}_x^{1/2}$ values approach to 0 as $\varepsilon=1$, as the ambient fluid flow is equal to the fluid flow at a stretching sheet, zero velocity gradient which corresponds to $C_f \, \mathrm{Re}_x^{1/2}$ is generated. The presence of nanoparticles theoretically increases the fluid friction with the surface. Evidently, the $C_f \, \mathrm{Re}_x^{1/2}$ of *SWCNT—Cu/water* hybrid nanofluid with 0.06 vol. *SWCNT* and 0.1 vol. *Cu* nanoparticles and the 0.16 vol. *Cu/water* nanofluid has more friction compared to 0.1 vol. of *Cu/water* nanofluid.

42

Nonetheless, the *SWCNT—Cu/water* hybrid nanofluid is about 10% of less fluid friction with the surface when comparing the result of 0.16 vol. *Cu/water* nanofluid at $\varepsilon = 5$. Less friction in *SWCNT—Cu/water* hybrid nanofluid is contributed by the less density of *SWCNT* nanoparticle as compared to the *Cu*.

Figure 4 demonstrate the variation of the surface temperature $\theta(0)$ for different values of the conjugate parameter γ. It can be seen in Figure 5 that the value of $\theta(0)$ rises as the value of γ increases. When conjugate parameter γ increases, the *SWCNT—Cu/water* hybrid nanofluid surface temperature $\theta(0)$ has increased substantially compared to both 0.1 and 0.16 vol. of *Cu* nanofluid. It also can be inferred that the nanoparticles volume fraction is affecting the $\theta(0)$ as the value increases in particular. Physically, the thermal conductivity of *SWCNT* is 16 times higher than *Cu*, thus provided the high values of $\theta(0)$ for the *SWCNT—Cu/water* hybrid nanofluid. The findings is in line with Arici (2001), as the influence of surface temperature on heat transfer characteristics is forecasted for the constant heat boundary condition using the nanoparticles volume fraction ratio as a parameter, and it is discovered that the conjugate parameter is also an effective parameter for the heat transfer properties.

The effect of the heat generation/absorption λ on the surface temperature $\theta(0)$ can be seen on Fig. 5. Each streamline contours do not vary very much from each other when $\lambda < -2$. It can be noticed that the *SWCNT-Cu/water* hybrid nanofluid surface temperature is remarkably increased as the heat coefficient is progressively increase as $\lambda > -2$. At, $\lambda = 0$ the value of $\theta(0)$ of *SWCNT-Cu/water* hybrid nanofluid is more than twice compared and 0.1 vol. of *Cu/water* nanofluid although there is slight difference for 0.16 vol. *Cu/water* nanofluid. Overall, *SWCNT-Cu/water* hybrid nanofluid has the highest $\theta(0)$ across the results. The heat is generated which causing the surface temperature rises. As a result, the rate of energy transmission is reduced, which is the polar opposite of heat absorption (Arici, 2001). Consequently, it can be deduced that heat absorption or generation has a considerable impact on nanofluid enhancement as $\lambda > -2$, since the heat conduction has a significant impact on nanofluid enhancement.

Figure 6—8 depicts temperature profiles $\theta(0)$ for various values of γ, λ and ε respectively. The presence of heat generation ($\lambda > 0$) aids in the growth of temperature profiles, as shown in the Figure 6. Due to the heat source adds more heat to the plate, the temperature profiles to rise. As a result, the thickness of the thermal boundary layer increases. Meanwhile, because heat is removed from the plate, the existence of heat absorption ($\lambda < 0$) causes the temperature profiles and boundary layer thickness to drop. This result is further supported by Bhattacharya et al. (2009), which found that when the temperature of the surface is lowered, the heat absorption/geneation coefficient increases, resulting in lower conductive thermal resistance.

In Figure 7, there are surface temperature variations across different values of conjugate parameters γ. It can be noted that the $\theta(0)$ is lower when the value of γ is higher. As the concentration of *SWCNT—Cu/water* hybrid nanoparticles increases, the surface temperature decreases, leads to an increase in heat transfer coefficient and, as a result, a decrease in convective thermal resistance.

The Figure 8 shows that there the ε affect the temperature and thermal boundary layer thickness. Essentially, as ε increases, the ratio of stretching to external velocity rises, enhancing the fluid's ability to rapidly move out from the stagnation region. The temperature of the plane's surface was reduced in regard to this condition.

43

Next, Figure 9 to 11 presents the velocity profiles $f'(\eta)$ for various values of γ, λ and ε respectively. From Fig. 9 and 10, the velocity profiles obtained is unique for various values of γ and λ. It is suggested that the increase in γ and λ did not effects the fluid velocity as well as its velocity boundary layer thicknesses. Physically, this provided the information that both parameters has no influenced on the skin friction coefficient. This can clearly explained by the equations 9 and 10 where the values of only affects the temperature and its heat transfer rate.

Lastly, the velocity profiles for various values of ε which yield $f'(0) = \varepsilon$ and $f'(\eta) = 1$ can be seen in Figure 11. When the value $\varepsilon > 1$, the flow has an inverted boundary layer structure, and the thickness of the boundary layer decreases as the value is increased. Furthermore, the flow has a boundary layer structure $a/b < 1$ will cause the external velocity of the surface bx exceeds the velocity of the stretching sheet. The thickness of the boundary layer will also increase in regards to increase of ε.

Conclusion

This paper investigates the heat generation/absorption on a stagnation point flow past a stretching sheet in *SWCNT—Cu/water* hybrid nanofluid with Newtonian heating by using numerical method. The velocity and temperature profiles, as well as the surface temperature, heat transfer coefficient, and skin friction coefficient, were all solved by using Runge-Kutta-Fehlberg (RKF45) method for various values of stretching parameter ε, conjugate parameter γ, heat generation/absorption coefficient parameter λ and the nanoparticle volume percentage for *SWCNT* ϕ_1 and *Cu* ϕ_2. It is discovered that as the stretching parameter is increased, the surface temperature and heat transfer coefficient will decline, whereas the conjugate parameter has the opposite effect.

After that, when *SWCNT* nanoparticles is introduced to the *Cu/water* nanofluid, the values of surface temperature and the heat transfer coefficient dramatically rise. The presence of heat generation aids in the increase of fluid temperature whilst the presence of heat absorption has the opposite or insignificant effect. It appears that the effects of hybrid nanoparticles are more substantial for lower stretching parameter and larger conjugate parameter values and heat generation/absorption, according to the numerical calculations. Finally, the fluid friction with the surface has grown as the nanoparticle volume fraction has increased.

Acknowledgments

References

Alkasasbeh, H. T., Abu-Ghurra, S., & Alzgool, H. A. (2019). Similarity solution of Heat Transfer for the Upper-Convected Maxwell Casson Fluid over a Stretching/Shrinking Sheet with Thermal Radiation. *JP Journal of Heat and Mass Transfer, 16*(1), 1-17.

Arici, M. (2001). Analysis of the conjugate effect of wall and flow parameters on pipe flow heat transfer. *Proceedings of the Institution of Mechanical Engineers, Part C: Journal of Mechanical Engineering Science, 215*(3), 307-313.

Bachok, N., Ishak, A., & Pop, I. (2011). Stagnation-point flow over a stretching/shrinking sheet in a nanofluid. *Nanoscale Research Letters, 6*(1), 1-10.

Bhattacharya, P., Samanta, A., & Chakraborty, S. (2009). Numerical study of conjugate heat transfer in rectangular microchannel heat sink with Al 2 O 3/H 2 O nanofluid. *Heat and Mass Transfer, 45*(10), 1323-1333.

Chamkha, A. J., El-Kabeir, S., & Rashad, A. (2015). Unsteady coupled heat and mass transfer by mixed convection flow of a micropolar fluid near the stagnation point on a vertical surface in the presence of radiation and chemical reaction. *Progress in Computational Fluid Dynamics, an International Journal, 15*(3), 186-196.

Chandrasekar, M., Suresh, S., & Bose, A. C. (2010). Experimental investigations and theoretical determination of thermal conductivity and viscosity of Al2O3/water nanofluid. *Experimental Thermal and Fluid Science, 34*(2), 210-216.

Choi, S., Zhang, Z. G., Yu, W., Lockwood, F., & Grulke, E. (2001). Anomalous thermal conductivity enhancement in nanotube suspensions. *Applied Physics Letters, 79*(14), 2252-2254.

Choi, S. U., & Eastman, J. A. (1995). *Enhancing thermal conductivity of fluids with nanoparticles*. Retrieved from

Crane, L. J. (1970). Flow past a stretching plate. *Zeitschrift für angewandte Mathematik und Physik ZAMP, 21*(4), 645-647.

Devi, S. U., & Devi, S. A. (2017). Heat transfer enhancement of cu− $ al_ {2} o_ {3} $/water hybrid nanofluid flow over a stretching sheet. *Journal of the Nigerian Mathematical Society, 36*(2), 419-433.

Eastman, J. A., Choi, U., Li, S., Thompson, L., & Lee, S. (1996). *Enhanced thermal conductivity through the development of nanofluids*. Retrieved from

Esfe, M. H., Alirezaie, A., & Rejvani, M. (2017). An applicable study on the thermal conductivity of SWCNT-MgO hybrid nanofluid and price-performance analysis for energy management. *Applied Thermal Engineering, 111*, 1202-1210.

Hamid, R. A., Nazar, R., & Pop, I. (2016). The non-alignment stagnation-point flow towards a permeable stretching/shrinking sheet in a nanofluid using Buongiorno's model: A revised model. *Zeitschrift für Naturforschung A, 71*(1), 81-89.

45

Hashim, H., Mohamed, M. K. A., Hussanan, A., Ishak, N., Sarif, N. M., & Salleh, M. Z. (2015). *The effects of slip conditions and viscous dissipation on the stagnation point flow over a stretching sheet.* Paper presented at the AIP Conference Proceedings.

Hayat, T., Imtiaz, M., & Alsaedi, A. (2016). Magnetohydrodynamic stagnation point flow of a Jeffrey nanofluid with Newtonian heating. *Journal of aerospace engineering, 29*(3), 04015063.

Hsiao, K.-L. (2016). Stagnation electrical MHD nanofluid mixed convection with slip boundary on a stretching sheet. *Applied Thermal Engineering, 98*, 850-861.

Ishak, N., Hussanan, A., Mohamed, M. K. A., Rosli, N., & Salleh, M. Z. (2019). *Heat and mass transfer flow of a viscoelastic nanofluid over a stretching/shrinking sheet with slip condition.* Paper presented at the AIP Conference Proceedings.

Li, C. H., & Peterson, G. (2006). Experimental investigation of temperature and volume fraction variations on the effective thermal conductivity of nanoparticle suspensions (nanofluids). *Journal of Applied Physics, 99*(8), 084314.

Mabood, F., Shateyi, S., Rashidi, M., Momoniat, E., & Freidoonimehr, N. (2016). MHD stagnation point flow heat and mass transfer of nanofluids in porous medium with radiation, viscous dissipation and chemical reaction. *Advanced Powder Technology, 27*(2), 742-749.

Merkin, J. (1994). Natural-convection boundary-layer flow on a vertical surface with Newtonian heating. *International Journal of Heat and Fluid Flow, 15*(5), 392-398.

Mohamed, M. K. A., Ismail, N. A., Hashim, N., Shah, N. M., & Salleh, M. Z. (2019). MHD slip flow and heat transfer on stagnation point of a magnetite (Fe3O4) ferrofluid towards a stretching sheet with Newtonian heating. *CFD Letters, 11*(1), 17-27.

Mohamed, M. K. A., Ong, H. R., Alkasasbeh, H. T., & Salleh, M. Z. (2020). *Heat Transfer of Ag-Al2O3/Water Hybrid Nanofluid on a Stagnation Point Flow over a Stretching Sheet with Newtonian Heating.* Paper presented at the Journal of Physics: Conference Series.

Noor, N., Haq, R. U., Nadeem, S., & Hashim, I. (2015). Mixed convection stagnation flow of a micropolar nanofluid along a vertically stretching surface with slip effects. *Meccanica, 50*(8), 2007-2022.

Sundar, L. S., Sharma, K., Singh, M. K., & Sousa, A. (2017). Hybrid nanofluids preparation, thermal properties, heat transfer and friction factor–a review. *Renewable and Sustainable Energy Reviews, 68*, 185-198.

Wang, X., Xu, X., & Choi, S. U. (1999). Thermal conductivity of nanoparticle-fluid mixture. *Journal of thermophysics and heat transfer, 13*(4), 474-480.

Xuan, Y., Li, Q., & Hu, W. (2003). Aggregation structure and thermal conductivity of nanofluids. *AIChE Journal, 49*(4), 1038-1043.

Yacob, N. A., Ishak, A., & Pop, I. (2011). Falkner–Skan problem for a static or moving wedge in nanofluids. *International Journal of Thermal Sciences, 50*(2), 133-139.

Yasin, S. H. M., Mohamed, M. K. A., Ismail, Z., Widodo, B., & Salleh, M. Z. (2019). Numerical solution on MHD stagnation point flow in ferrofluid with Newtonian heating and thermal radiation effect. *Journal of Advanced Research in Fluid Mechanics and Thermal Sciences, 57*(1), 12-22.

Zhu, H., Zhang, C., Liu, S., Tang, Y., & Yin, Y. (2006). Effects of nanoparticle clustering and alignment on thermal conductivities of Fe 3 O 4 aqueous nanofluids. *Applied Physics Letters, 89*(2), 023123.

How to cite this paper: Abdul Muiz Mohd Zaki, Nurul Farahain Mohammad, Siti Khuzaimah Soid, Muhammad Khairul Anuar Mohamed, Rahimah Jusoh (2021). Effects of Heat Generation/Absorption on a Stagnation Point Flow Past a Stretching Sheet Carbon Nanotube Water-Based Hybrid Nanofluid with Newtonian Heating. *Malaysian Journal of Applied Sciences, 6*(2), 34-47.